PHYSICAL REVIEW B **91**, 020101(R) (2015)

Prediction of a stable post-post-perovskite structure from first principles

Changsong Xu,[1,2] Bin Xu,[2] Yurong Yang,[2] Huafeng Dong,[3] Artem R. Oganov,[3,4,5] Shanying Wang,[1] Wenhui Duan,[1,6] Binglin Gu,[6] and L. Bellaiche[2]

[1]*State Key Laboratory of Low-Dimensional Quantum Physics and Collaborative Innovation Center of Quantum Matter, Department of Physics, Tsinghua University, Beijing 100084, China*

[2]*Physics Department and Institute for Nanoscience and Engineering, University of Arkansas, Fayetteville, Arkansas 72701, USA*

[3]*Department of Geosciences, Center for Materials by Design and Institute for Advanced Computational Science, State University of New York, Stony Brook, New York 11794, USA*

[4]*Moscow Institute of Physics and Technology, 9 Institutskiy Lane, Dolgoprudny City, Moscow Region 141700, Russia*

[5]*School of Materials Science, Northwestern Polytechnical University, Xi'an 710072, China*

[6]*Institute for Advanced Study, Tsinghua University, Beijing 100084, China*

(Received 27 August 2014; revised manuscript received 12 November 2014; published 15 January 2015)

A novel stable crystal structure is discovered in a variety of ABO_3, ABF_3, and A_2O_3 compounds, via the use of first principles. This novel structure appears under hydrostatic pressure, and can be considered to be a post-post-perovskite phase. It provides a successful solution to experimental puzzles in important systems and is characterized by one-dimensional channels linked by a group of two via edge-sharing oxygen/fluorine octahedra. Such organization automatically results in anisotropic elastic properties and new magnetic arrangements. Depending on the system of choice, this post-post-perovskite structure also possesses electronic band gaps ranging from zero to $\simeq$10eV being direct or indirect in nature.

DOI: 10.1103/PhysRevB.91.020101 PACS number(s): 61.50.Ks, 71.20.−b, 75.25.−j

ABX_3 perovskites (Pv) form an important class of crystal structures for which A and B are cations and X is typically the oxygen or fluorine anion. Perovskites display a wealth of phenomena, such as ferroelectricity, magnetism, multiferroicity, piezoelectricity, magneto-electricity, charge and orbital orderings, superconductivity, etc. As a result, they constitute a rich playground for research and are important for various technologies, which explains the flurry of activities that have been devoted to them [1]. Interestingly, recent works have shown that applying a hydrostatic pressure in some ABX_3 materials can result in the transformation from the Pv structure to the so-called "post-perovskite" (pPv) structure, which can have important physical consequences [2–9]. For instance, the pPv structure discovered in $MgSiO_3$ explains the existence of anisotropic features in the D" layer of Earth [8–10]. Moreover, $CaRhO_3$ was recently found to adopt a polymorph that was described as being an intermediate phase between perovskite and post-perovskite [11]. Based on these discoveries as well as recent findings of new high-pressure phases in ABO_3 and ABF_3 systems [12–14], one may wonder if there is another crystal structure (to be termed as "post-post-perovkite" (ppPv)) for which Pv or pPv materials can evolve to under hydrostatic pressure. Positively answering such question will deepen the current knowledge of crystallography and high pressure. Moreover, if such structure does exist, one may also wonder about its structural characteristics and if they can lead to novel physical properties—which is obviously interesting for fundamental reason but also for the design of original devices. It is also of high importance to determine what precise compounds may possess such hypothetical structure.

The goal of this Rapid Communication is to address all these aforementioned unknown questions, via the use of first-principles calculations. As we will see, surprises are in store since we, e.g., (1) predict that many and various ABX_3 and A_2O_3 materials can transform to a common, novel, and stable ppPv structure (from a pPv structure or even directly from a Pv structure) under hydrostatic pressure; and (2) reveal its unusual structural, magnetic, and electronic properties. Moreover, this ppPv structure is likely the "N phase" that has been observed in Refs. [2,3].

As detailed in Ref. [15] (see, also, Refs. [2,3,8–11,16–39] therein), first-principles calculations are performed on many ABX_3 and A_2O_3 materials, with different A and B atoms and with X = O or F anion, under hydrostatic pressure. A list of these materials is indicated in Fig. 1.

Crystal structures. Let us first concentrate on a specific material that has been experimentally explored under pressure, namely $NaMgF_3$. Figure 2(a) shows that the orthorhombic Pv $Pnma$ phase (Pv-$Pnma$) is predicted to be its ground state up to $\simeq$20 GPa, as consistent with measurements [2,3,40]. Such phase is common to many perovskites [20] and is schematized in Fig. 2(b). In this phase, any fluorine (or oxygen) octahedra share corners with their neighboring octahedra along the pseudocubic [100], [010], and [001] directions. Figure 2(a) further reveals that $NaMgF_3$ is predicted to experience a phase transition to the (orthorhombic) *post-perovskite* $Cmcm$ phase (pPv-$Cmcm$) at $\simeq$20 GPa, for which not only the space group but also the crystal structure change, as schematized in Fig. 2(c). Interestingly, the Pv-$Pnma$–to–pPv-$Cmcm$ transition has been observed to occur for pressure around 27–30 GPa and under laser heating (likely, to overcome the kinetic barrier inherent to first-order transitions) [2,3] in $NaMgF_3$, which is rather consistent with our prediction of a corresponding critical pressure of $\simeq$20 GPa at 0 K. As indicated by Fig. 3 and Table I of the Supplemental Material (SM) [15], the pPv-$Cmcm$ phase differs from the Pv-$Pnma$ structure by the existence of two-dimensional sheets formed by octahedra that share edges along the a axis and corners along the c axis. These two-dimensional sheets are stacked along the b axis with an interlayer made of A atoms separating any two neighboring sheets. As a result, the elastic (stiffness) constant of pPv-$Cmcm$ is much lower along the b axis than along

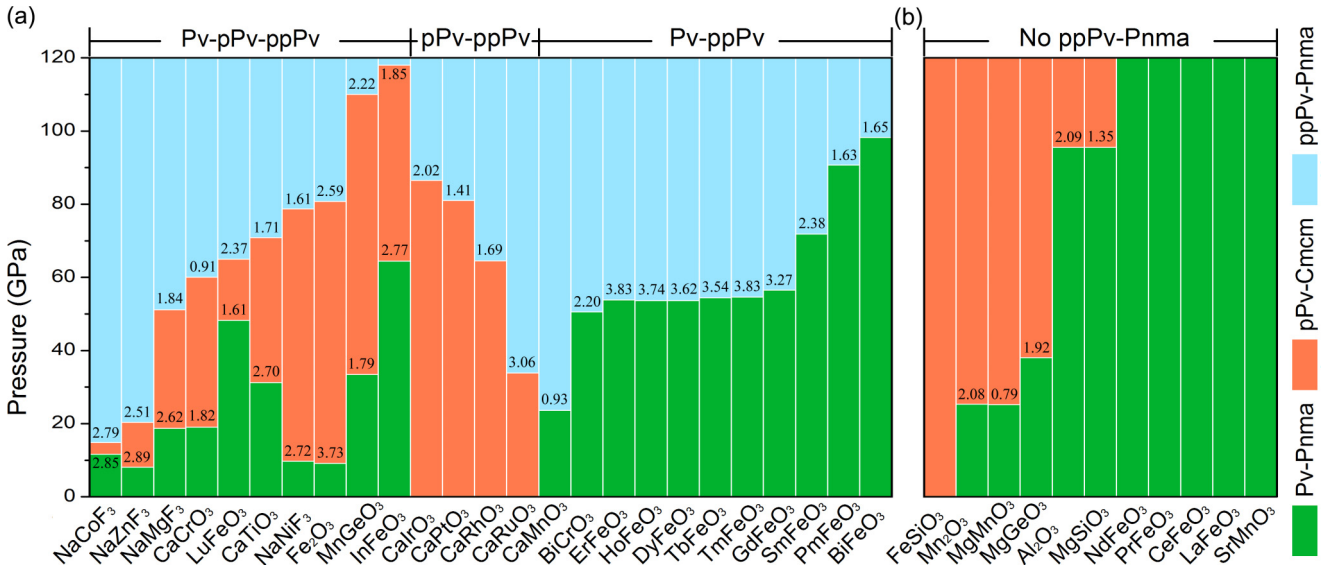

FIG. 1. (Color online) Pressure range of stability of the Pv-*Pnma*, pPv-*Cmcm*, and ppPv-*Pnma* phases in the ABX_3 and A_2O_3 materials under study. (a) and (b) report materials possessing or missing, respectively, the presently discovered ppPv-*Pnma* structure for pressure up to 120 GPa. Numbers in these panels indicate the decrease in volume (in percentage) at the transitions.

the *a* or *c* axis for any material, including $NaMgF_3$ (see Table II of the SM [15] and $MgSiO_3$—which, for this latter compound, is consistent with the seismic anisotropy observed in the so-called D" layer of Earth [8,10].

As also revealed by Fig. 2(a), we further found that $NaMgF_3$ undergoes another transition at $\simeq$51 GPa, for which the space group and crystal structure both change again: the resulting phase re-adopts the *Pnma* space group but within a different crystal structure that is termed "post-post-perovskite" [3,41,42] and that is denoted as ppPv-*Pnma* in the following. Its structural characteristics are shown in Figs. 2(d) and 2(e). Interestingly, while ppPv-*Pnma* has never been previously reported in any material, its present discovery solves a puzzle: it likely is the so-called "N phase" that has been observed in Refs. [2,3], based on the facts that (i) it experimentally appears as a result of a phase transformation from the pPv-*Cmcm* phase at 56 GPa under laser-heating of about 2000 K (as consistent with our predicted pPv-*Cmcm*–to–ppPv-*Pnma* transition for a critical pressure $\simeq$51 GPa at T = 0 K); (ii) the N phase has been assigned an orthorhombic symmetry [2], in line with the *Pnma* space group we presently found for our ppPv structure [43]; and (iii) our simulated x-ray diffraction pattern of ppPv-*Pnma* is consistent with the one experimentally found in Ref. [3] for this N phase (see Fig. 4 of Ref. [15]).

Remarkably, comparing Figs. 2(c) with 2(d) and 2(e) reveals that the transformation from pPv-*Cmcm* to ppPv-*Pnma* results in the breaking of the two-dimensional octahedra sheet at the shared corners in favor of one-dimensional channels that are elongated along the *b* axis of the ppPv-*Pnma* structure. These channels organize themselves by group of two (with the two channels forming the double channel being parallel to each other along the *b* axis), as a result of edge-sharing octahedra. As shown in Table I of the SM [15], for a given pressure of 60 GPa (which is rather close to the predicted pPv-*Cmcm*–to–ppPv-*Pnma* transition), the formation of these double channels leads, in $NaMgF_3$, to the *b* and *c* lattice constants of ppPv-*Pnma* being larger by 4.3% and 25.3%, respectively, than the *a* and *b* lattice constants of pPv-*Cmcm*. On the other hand, the *a* lattice parameter of ppPv-*Pnma* is smaller by 24.9% than the *c* lattice constant of pPv-*Cmcm* [note that the *b* axis is parallel to the direction of the one-dimensional channel in ppPv-*Pnma* while it is perpendicular to the octahedra sheets in pPv-*Cmcm*, implying that comparisons have to be made between the (*a*,*b*,*c*) triad axis of ppPv-*Pnma* and the (*c*,*a*,*b*) triad axis of pPv-*Cmcm*]. As shown in the inset of Fig. 2(a), such changes in lattice constants result in a decrease of 1.84% of the volume at the pPv-*Cmcm*–to–ppPv-*Pnma* transition in $NaMgF_3$, which is a prediction that can be easily checked by measurements. Note that the octahedra are more distorted in ppPv-*Pnma* than in pPv-*Cmcm*, as evidenced by the facts that the six Mg-F bonds of the octahedra in ppPv-*Pnma* adopt four different values equal to 1.813, 1.871 (doubly degenerate), 1.888 (doubly degenerate), and 1.942 Å, respectively, while those of pPv-*Cmcm* only split between two values of 1.785 (doubly degenerate) and 1.846 Å (four times degenerate), respectively, for a pressure of 60 GPa. The fluorine octahedra therefore become 0.84% larger in ppPv-*Pnma* than in pPv-*Cmcm* (even if the volume decreases), as edge-sharing allows for more compact packing. Moreover, in the ppPv-*Pnma* phase, any Mg ion belonging to one channel gets rather close to a specific F ion belonging to the adjacent channel [indicated by the dashed line in Fig. 2(d)] forming the double channels and therefore leads to an increase in coordination number from 6 to "6+1." For instance, at 60 GPa, the bond between these Mg and specific F ions is about 2.103 Å, which is comparable to the distances of 1.813–1.942 Å between Mg and F ions belonging to the same octahedra [44].

Figure 1(a) also shows that many materials are also predicted to exhibit the aforementioned Pv-*Pnma*–to–pPv-*Cmcm* and pPv-*Cmcm*–to–ppPv-*Pnma* transitions, but at different critical pressures. On the other hand, Fig. 1(a)

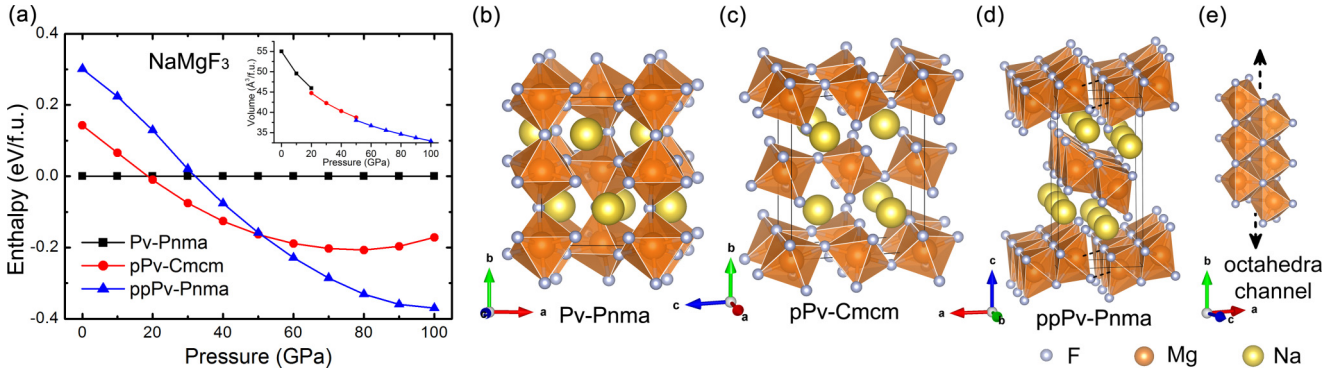

FIG. 2. (Color online) Pressure dependence of the enthalpy of the Pv-*Pnma*, pPv-*Cmcm*, and ppPv-*Pnma* phases of $NaMgF_3$ (a), along with the schematization of (b) the Pv-*Pnma*, (c) pPv-*Cmcm*, and [(d) and (e)] ppPv-*Pnma* crystal structures. Note that the enthalpy of the Pv-*Pnma* phase has been set to be zero for any pressure in (a), and that the inset in (a) displays the behavior of the volume vs pressure in the Pv-*Pnma*, pPv-*Cmcm*, and ppPv-*Pnma* phases (in the pressure ranges they have the lowest enthalpy).

further indicates that some materials are predicted to *directly* transform from Pv-*Pnma* to ppPv-*Pnma* without adopting the intermediate pPv-*Cmcm* phase, as the pressure increases. Examples include (i) $BiFeO_3$ and $BiCrO_3$ that are often studied for their multiferroic properties [45,46]; (ii) $CaMnO_3$ that has been predicted to exhibit both magnetic and electric orderings when grown as a strained film [47,48]; and (iii) the rare-earth ferrites $RFeO_3$ [28–30] with small or intermediate ionic radius. For instance and as shown in Fig. 1(a) of Ref. [15], $GdFeO_3$ directly undergoes a transition from Pv-*Pnma* to ppPv-*Pnma* at the pressure of $\simeq 56.5$ GPa. Conversely, there are some materials, such as $CaBO_3$ with $B =$ Ru, Ir, Rh, Pt (that have been investigated because of their analogy with $MgSiO_3$ [4–7,49,50] or because of the strong effect of spin orbit interactions on some of their physical properties [51]) that do not exhibit the Pv-*Pnma* phase but rather evolve from pPv-*Cmcm* to ppPv-*Pnma*, as a hydrostatic pressure is applied and increased (see Fig. 1(b) of Ref. [15] for $CaPtO_3$). In particular, we predict that the ppPv-*Pnma* phase of $CaRuO_3$ will appear at a pressure of 33.8 GPa, which should make its observation rather easily feasible. Note that Fig. 1 also indicates that the volume is typically reduced by an amount varying between 0.9% and 3.8% (depending on the chemistry) at the critical pressure at which the post-post-perovskite structure becomes the most stable phase in our studied compounds. Moreover and as shown in Fig. 1(b), no ppPv structure was found *up to 120 GPa* in some other systems, such as $RFeO_3$ compounds with large ionic radius (i.e., $R =$ Nd, Pr, Ce, and La, see Fig. 1(c) of Ref. [15]), $MgSiO_3$, Mn_2O_3, or Al_2O_3—as consistent with measurements and previous computations [8,9,32–34] (note that Ref. [15] provides a more detailed comparison between our predictions and these previous works).

Dynamical stability. The ppPv-*Pnma* structure is *dynamically* stable in its pressure range of stability for all the materials shown in Fig. 1(a). Two examples are shown in Figs. 2(a) and 2(c) of Ref. [15] for $NaMgF_3$ and $GdFeO_3$, respectively, both under a pressure of 60 GPa. In fact, we also numerically found that, in several studied compounds, ppPv-*Pnma* does not have any unstable phonon even in pressure regions for which this phase is not the lowest one in enthalpy. For instance and as shown in Fig. 1(b) of Ref. [15], ppPv-*Pnma* is dynamically stable even at zero pressure in, e.g., $CaPtO_3$. As consistent with previous works [52,53], this stability likely implies that this phase can be quenched to ambient pressure in this material (especially because the difference in enthalpy between pPv-*Cmcm* and ppPv-*Pnma* is found to be as small as 181 meV/5-atom at zero pressure in $CaPtO_3$). Conversely, other phases, such as pPv-*Cmcm*, can also have no unstable phonon in the pressure range for which ppPv-*Pnma* has the lowest enthalpy, which implies that (i) pPv-*Cmcm* may still be experimentally found in some materials at pressure higher than the predicted pPv-*Cmcm*–to–ppPv-*Pnma* transition pressure and (ii) observing ppPv-*Pnma* phase in these materials may require the use of laser heating (to overcome kinetic barrier). Note that the aforementioned Pv-*Pnma*–to–pPv-*Cmcm* and pPv-*Cmcm*–to–ppPv-*Pnma* transitions are of reconstructive type, and that the Pv-*Pnma*, pPv-*Cmcm* and ppPv-*Pnma* phases form local minima that are linked by bond-breaking, which explains their dynamical stability.

Electronic structure. We also numerically found that within ppPv-*Pnma*, the *electronic* band gap can be rather quantitatively different between investigated materials (see Table III and Fig. 2 of Ref. [15]). For instance, the calculated band gap of $NaMgF_3$ is as large as 9.04 eV for a pressure of 60 GPa while it is dramatically reduced to 0.83 eV for $GdFeO_3$ under the same pressure. In fact, a few systems are even metallic above the pressure at which the ppPv-*Pnma* phase begins to appear. Examples include $CaRhO_3$ at 70 GPa and $CaIrO_3$ at 90 GPa. Equally striking and as shown in Fig. 2 of Ref. [15] too, even the character of the band gap (that is direct *versus* indirect) can be altered when going from one material to another within ppPv-*Pnma*. Such electronic flexibility may result, in the future, to the discovery of anomalous properties (such as metal-insulator transitions [54]) or highly-desired features (such as a direct-band gap in the frequency spectrum needed for photovoltaic devices [55] or light-emitting devices [56]) in materials possessing the ppPv-*Pnma* structure.

Magnetic ordering. Interestingly, some ABO_3 materials, that are predicted to exhibit ppPv-*Pnma* structure, possess A and/or B atoms that are *magnetic*. As a result, novel or striking magnetic arrangements should emerge, especially when recalling that ppPv-*Pnma* adopts unusual "double"

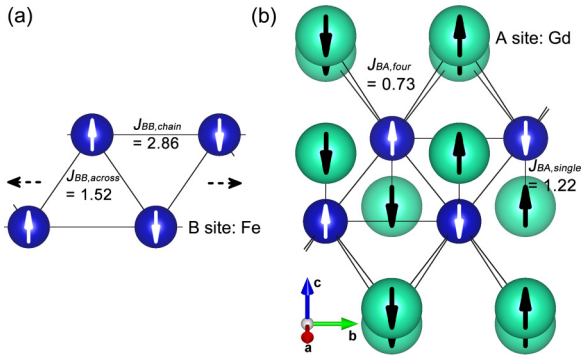

FIG. 3. (Color online) Magnetic ground state of the ppPv-*Pnma* phase of $GdFeO_3$ under 60 GPa. (a) The strength of the magnetic interactions and the resulting magnetic ordering between Fe ions, (b) the coupling coefficients associated with Fe and Gd magnetic interactions as well as the spin pattern adopted by these two types of ions.

one-dimensional channels inside which A and B bond with O atoms [see Figs. 2(d) and 2(e)]. Let us, for instance, consider the case of the ppPv-*Pnma* phase of $GdFeO_3$ at 60 GPa and include the $4f$ electrons of Gd in the valence in the calculations, thus allowing both Gd and Fe ions to adopt localized magnetic moments (that are found to be 6.90 μ_B and 4.12 μ_B, respectively). Practically, enthalpies of different collinear magnetic configurations are computed and used to extract the coupling coefficients ($J_{BB,\text{chain}}$, $J_{BB,\text{across}}$, $J_{BA,\text{single}}$, $J_{BA,\text{four}}$) of the model described by $H = \frac{1}{2}J_{BB,\text{chain}}\sum_{i,j}\boldsymbol{S}_i\cdot\boldsymbol{S}_j + \frac{1}{2}J_{BB,\text{across}}\sum_{i,j}\boldsymbol{S}_i\cdot\boldsymbol{S}_j + \frac{1}{2}J_{BA,\text{single}}\sum_{i,j}\boldsymbol{S}_i\cdot\boldsymbol{S}_j + \frac{1}{2}J_{BA,\text{four}}\sum_{i,j}\boldsymbol{S}_i\cdot\boldsymbol{S}_j$, where the sums over i run over all Fe atoms, while the first (respectively, last) two sums over j run over specific Fe (respectively, Gd) atoms that will be indicated below. As depicted in Fig. 3, the strongest coupling coefficient (denoted by $J_{BB,\text{chain}}$) is found to be 2.86 meV (that is antiferromagnetic in nature) and is between Fe ions that are distant (by $\simeq$3.02 Å) along the b axis. Interestingly, the coupling between Fe ions that belong to two adjacent and parallel one-dimensional channels (and are distant by $\simeq$2.67 Å) is also antiferromagnetic in nature but is of smaller magnitude since it is equal to 1.52 meV (this parameter is denoted here as $J_{BB,\text{across}}$). As a result and as shown in Fig. 3(a), the magnetic ground state of $GdFeO_3$ possesses one-dimensional antiferromagnetic chains elongating along the b axis and formed by Fe ions with each of these Fe ions having two neighboring Fe ions of opposite spins and that belong to the adjacent parallel chain. Note that the particular *triangularlike* geometry seen by any magnetic B ion [see Fig. 3(a)] because of the formation of the double one-dimensional channels inherent to ppPv-*Pnma* in ABO_3 materials is a perfect "recipe" to generate the so-called *geometric frustration* [57,58] in the specific (and presently hypothetical) case that $J_{BB,\text{chain}}$ and $J_{BB,\text{across}}$ would still be antiferromagnetic in nature but would now be close to each other in magnitude (unlike in $GdFeO_3$). Searching for such compounds or the hypothetical pressure giving rise to such condition in some materials therefore constitutes a promising avenue to pursue in the future. Note also that we numerically found that, in the ppPv-*Pnma* phase of $GdFeO_3$ at 60 GPa, magnetic interactions between Gd ions are negligible (as consistent with the deep f shell of Gadolinium) but Fe ions are antiferromagnetically coupled with their closest Gd ions. As indicated in Fig. 3(b), the resulting coupling is $J_{BA,\text{single}} = 1.22$ meV between Fe and Gd ions that form single bond (and are distant by 2.783 Å) while it is $J_{BA,\text{four}} = 0.73$ meV between Fe and Gd ions that are tetrahedrally bonded (and distant by 3.121 Å). As a result, the magnetic ordering of Gd ions is governed by their interaction with Fe ions and is the one depicted in Fig. 3(b).

In summary, we used first-principles techniques to discover a common and stable ppPv crystal structure in a variety of ABX_3 and A_2O_3 materials under pressure. Such phase exhibits one-dimensional structural characteristics that naturally lead to strong anisotropy and novel magnetic orderings, and provides a plausible explanation for the N phase that has been reported in Refs. [2,3]. Moreover, the electronic band gap of this phase is highly dependent on the system and can be of rather different nature and magnitude. We hope that this Communication will encourage researchers to confirm the predictions presently reported and to determine properties associated with such novel crystal structure.

Acknowledgments. This work is financially supported by the Department of Energy, Office of Basic Energy Sciences, under contract ER-46612 (B.X.), ONR Grant N00014-12-1-1034 (Y.Y.), and NSF grant DMR-1066158 (L.B.). It is also supported by the Ministry of Science and Technology of China (Grant No. 2011CB606405) and National Natural Science Foundation of China (Grant No. 11174173). A.O. thanks the National Science Foundation (EAR-1114313, DMR-1231586), DARPA (Grants No. W31P4Q1210008 and No. W31P4Q1310005), the Government of Russian Federation (Grant 14.A12.31.0003) of Russian Federation, and Foreign Talents Introduction and Academic Exchange Program (No. B08040). The calculations were performed on the "Razor" (University of Arkansas) and "Explorer 100" (Tsinghua University) cluster systems.

[1] A. S. Bhalla, R. Guo, and R. Roy, Material Res. Innov. **4**, 3 (2000).

[2] C. D. Martin, W. A. Crichton, H. Liu, V. Praparkenka, J. Chen, and J. B. Parise, Am. Mineral. **91**, 1703 (2006).

[3] C. D. Martin, W. A. Crichton, H. Liu, V. Praparkenka, J. Chen, and J. B. Parise, Geophys. Res. Lett. **33**, L11305 (2006).

[4] C. L. McDaniel and S. J. Schneider, J. Solid State Chem. **4**, 275 (1972).

[5] H. Kojitani, Y. Shirako, and M. Akaogi, Phys. Earth Planet. Inter. **165**, 127 (2007).

[6] Y. Shirako, H. Kojitani, M. Akaogi, K. Yamaura, and E. Takayama-Muromachi, Phys. Chem. Miner. **36**, 455 (2009).

[7] K. Ohgushi, Y. Matsushita, N. Miyajima, Y. Katsuya, M. Tanaka, F. Izumi, H. Gotou, Y. Ueda, and T. Yagi, Phys. Chem. Miner. **35**, 189 (2008).

[8] A. R. Oganov and S. Ono, Nature (London) **430**, 445 (2004).

[9] M. Murakami, K. Hirose, K. Kawamura, N. Sata, and Y. Ohishi, Science **304**, 855 (2004).
[10] A. R. Oganov, R. Martonak, A. Laio, P. Raiteri, and M. Parrinello, Nature (London) **438**, 1144 (2005).
[11] Y. Shikaro *et al.*, Am. Mineral. **97**, 159 (2012).
[12] L. Zhang *et al.*, Science **344**, 877 (2014)
[13] R. E. Cohen and Y. Lin, Phys. Rev. B **90**, 140102 (2014).
[14] W. A. Crichton, F. L. M. Bernal, J. Guignard, M. Hanfland, and S. Margadonna, arXiv:1410.2783
[15] See Supplemental Material at http://link.aps.org/supplemental/10.1103/PhysRevB.91.020101 for details about the methods used, as well as additional information.
[16] A. R. Oganov and C. W. Glass, J. Chem. Phys. **124**, 244704 (2006).
[17] A. O. Lyakhov, A. R. Oganov, H. T. Stokes, and Q. Zhu, Comput. Phys. Commun. **184**, 1172 (2013).
[18] A. R. Oganov, A. O. Lyakhov, and M. Valle, Acc. Chem. Res. **44**, 227 (2011).
[19] A. R. Oganov, Y. Ma, A. O. Lyakhov, M. Valle, and C. Gatti, Rev. Mineral. Geochem. **71**, 271 (2010).
[20] J. Zhao, N. L. Ross, and R. J. Angel, Acta Cryst. B **60**, 263 (2004), and references therein.
[21] G. Kresse and D. Joubert, Phys. Rev. B **59**, 1758 (1999).
[22] J. P. Perdew, A. Ruzsinszky, G. I. Csonka, O. A. Vydrov, G. E. Scuseria, L. A. Constantin, X. Zhou, and K. Burke, Phys. Rev. Lett. **100**, 136406 (2008).
[23] O. Diéguez, O. E. González-Vázquez, J. C. Wojdel, and J. Íñiguez, Phys. Rev. B **83**, 094105 (2011).
[24] P. E. Blochl, Phys. Rev. B **50**, 17953 (1994).
[25] A. Togo, F. Oba, and I. Tanaka, Phys. Rev. B **78**, 134106 (2008).
[26] W. S. Choi, D. G. Kim, S. S. A. Seo, S. J. Moon, D. Lee, J. H. Lee, H. S. Lee, D.-Y. Cho, Y. S. Lee, P. Murugavel, J. Yu, and T. W. Noh, Phys. Rev. B **77**, 045137 (2008).
[27] P. Xiao, J.-G. Cheng, J.-S. Zhou, J. B. Goodenough, and G. Henkelman, Phys. Rev. B **88**, 144102 (2013).
[28] R. L. White, J. Appl. Phys. **40**, 1061 (1969).
[29] H. J. Zhao, W. Ren, Y. Yang, X. Chen, and L. Bellaiche, J. Phys.: Condens. Matter **25**, 466002 (2013).
[30] C. Xu, Y. Yang, S. Wang, W. Duan, B. Gu, and L. Bellaiche, Phys. Rev. B **89**, 205122 (2014).
[31] S. Yakovlev, M. Avdeev, and M. Mezouar, J. Solid State Chem. **182**, 1545 (2009).
[32] J. Santillan and S. H. Shim, AGU Fall Meeting No. MR23B-0050 (2005).
[33] S. Ono, A. R. Oganov, T. Koyama, and H. Shimizu, Earth Planet. Sci. Lett. **246**, 326 (2006).
[34] R. Caracas and R. E. Cohen, Geophys. Res. Lett. **32**, L16310 (2005).
[35] K. Umemoto, R. M. Wentzcovitch, and P. B. Allen, Science **311**, 983 (2006).
[36] K. Umemoto, R. M. Wentzcovitch, D. J. Weidner, and J. B. Parise, Geophys. Res. Lett. **33**, L15304 (2006).
[37] B. Grocholski, S.-H. Shim, and V. B. Prakapenka, Geophys. Res. Lett. **37**, L14204 (2010).
[38] F. Gao, Y. Yuan, K. F. Wang, X. Y. Chen, J.-M. Liu, and Z. F. Ren, Appl. Phys. Lett. **89**, 102506 (2006).
[39] A. V. Krukau, O. A. Vydrov, A. F. Izmaylov, and G. E. Scuseria, J. Chem. Phys. **125**, 224106 (2006).
[40] M. OKeeffe, B. G. Hyde, and Bovin, Phys. Chem. Minerals **4**, 299 (1979).
[41] R. Caracas and R. E. Cohen, Phys. Rev. B **76**, 184101 (2007).
[42] H. Yusa, Y. Shirako, M. Akaogi, H. Kojitani, N. Hirao, Y. Ohishi, and T. Kikegawa, Inorg. Chem. **51**, 6559 (2010).
[43] Note, however, that Ref. [2] tentatively assigns a *Pnnm* space group rather than *Pnma* for their N phase. It will thus be interesting if the authors of Ref. [2] can check if *Pnma* better describes their experimental data, especially once realizing that *Pnnm* and *Pnma* share the same *mmm* point group.
[44] Note that, for comparison, the closest distance between Mg and F ions that do not belong to the same octahedra is about 2.929 Å in the pPv-*Cmcm* phase at around 60 GPa, while the distances between Mg and F ions belonging to the same octahedra range between 1.785 and 1.846 Å.
[45] J. Wang, J. B. Neaton, H. Zheng, V. Nagarajan, S. B. Ogale, B. Liu, D. Viehland, V. Vaithyanathan, D. G. Schlom, U. V. Waghmare, N. A. Spaldin, K. M. Rabe, M. Wuttig, and R. Ramesh, Science **299**, 1719 (2003).
[46] M. Murakami, S. Fujino, S.-H. Lim, C. J. Long, L. G. Salamanca-Riba, M. Wuttig, I. Takeuchi, V. Nagarajan, and A. Varatharajan, Appl. Phys. Lett. **88**, 152902 (2006).
[47] S. Bhattacharjee, E. Bousquet, and P. Ghosez, Phys. Rev. Lett. **102**, 117602 (2009).
[48] E. Bousquet and N. Spaldin, Phys. Rev. Lett. **107**, 197603 (2011).
[49] K. Hirose and Y. Fujita, Geophys. Res. Lett. **32**, L13313 (2005).
[50] Y. Inaguma, K. Hasumi, M. Yoshida, T. Ohba, and T. Katsumata, Inorg. Chem. **47**, 1868 (2008).
[51] K. Ohgushi, J. I. Yamaura, H. Ohsumi, K. Sugimoto, S. Takeshita, A. Tokuda, H. Takagi, M. Takata, and T. H. Arima, Phys. Rev. Lett. **110**, 217212 (2013).
[52] Y. Shirako, Y. G. Shi, A. Aimi, D. Mori, H. Kojitani, K. Yamaura, Y. Inaguma, and M. Akaogi, J. Solid State Chem. **191**, 167 (2012).
[53] A. C. Garcia-Castro, A. H. Romero, and E. Bousquet, Phys. Rev. B **90**, 064113 (2014).
[54] M. Imada, A. Fujimori, and Y. Tokura, Rev. Mod. Phys. **70**, 1039 (1998).
[55] J. M. Pearce, Futures **34**, 663 (2012).
[56] J. H. Burroughes, D. D. C. Bradley, A. R. Brown, R. N. Marks, K. Mackay, R. H. Friend, P. L. Burns, and A. B. Holmes, Nature (London) **347**, 539 (1990).
[57] R. Moessner and R. P. Ramirez, Phys. Today **59**, 24 (2006).
[58] N. Choudhury, L. Walizer, S. Lisenkov, and L. Bellaiche, Nature (London) **470**, 513 (2011).